Macromolecules

ARTICLE

pubs.acs.org/Macromolecules

Synthesis, Characterization, and Gas Separation Properties of Novel Copolyimides Containing Adamantyl Ester Pendant Groups

E. M. Maya,* I. García-Yoldi, A. E. Lozano, J. G. de la Campa, and J. de Abajo

Departamento de Química Macromolecular Aplicada, Instituto de Ciencia y Tecnología de Polímeros, CSIC, Juan de la Cierva 3, 28006 Madrid, Spain

ABSTRACT:

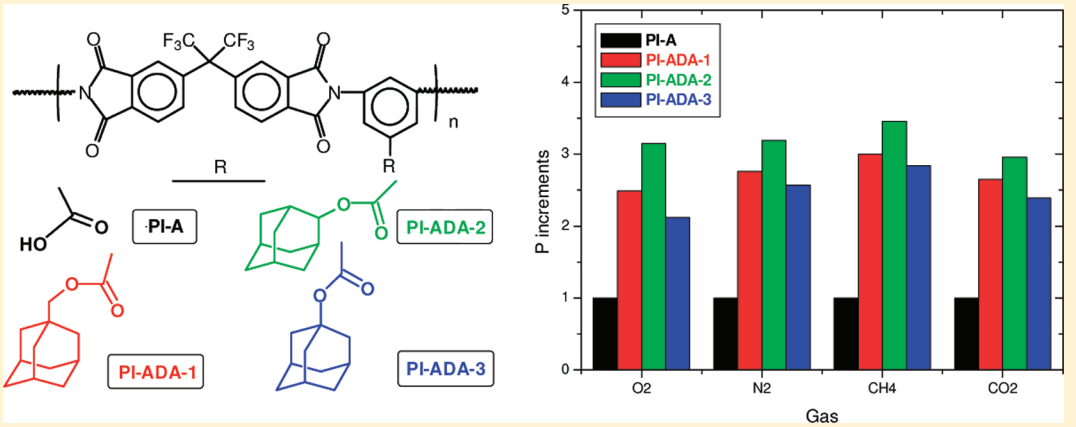

This paper reports the synthesis and characterization of a novel family of copolyimides having adamantyl ester pendant groups, along with their characterization and a study of properties such as solubility, thermal stability, and gas separation capacity. The incorporation of the pendant groups was done through esterification reactions using a copolyimide with free −COOH pendant groups and three adamantane−alcohols with different substitutions. The gas permeation (P) and diffusion (D) coefficients of the three copolyimides were higher than the starting copolyimide and they were governed by the fractional free volume, which confirmed the positive effect of adamantane groups on reducing the molecular packing and therefore increasing P and D. To confirm the above statement, theoretical fractional free volume, density and free volume distribution were calculated observing similar trends to those obtained experimentally. Finally, evaluation of $P(CO_2)$ behavior as a function of CO_2 feed pressure revealed the absence of plasticization, what was attributed to the film densification caused by the thermal annealing.

INTRODUCTION

It is well-known that aromatic polyimides have good gas permeation properties as well as excellent thermal and mechanical properties.[1] Their gas permeation properties have been improved by modification of their chemical structure, for example, introducing bulky side substituents[2] that hinders the molecular packing and reduces the rotational mobility of the main chain.

Adamantane is a bulky diamond-like cage structure composed of three fused cyclohexane rings arranged in a chair conformations which results in a large structure (volume higher than 150 Å^3, Figure 1), which tends to inhibit the packing of polymer chains and to decrease the polymer crystallinity, what is translated into an improved processability.[3] Thus, adamantane should be considered as a good substituent to improve the gas transport properties of polyimides.

The incorporation of adamantane groups into aromatic polymers has been previously reported to improve polymer solubility or to enhance dielectric properties while maintaining the thermal properties. Thus, Espeso et al., have reported aromatic polyisophthalamides containing adamantyl pendant groups which showed good solubility, good thermal resistance and exceptionally high glass transition temperatures.[4] Chern et al.[5−8] and Matheus et al.[9−11] have studied the thermal and dielectric properties of polyimides containing adamantane groups in the main chain. They found that most of these polyimides exhibited low dielectric constant (2.4 to 2.9) and good thermal resistance with no weight loss up to 350 °C. Other authors have explored the incorporation of adamantyl moieties into polyimides as pendant groups.[12−16] These polyimides exhibited high glass transition temperatures, between 250 and 330 °C, good thermal stability up to 400 °C, and excellent solubility in common organic solvents such as tetrahydrofuran and chloroform.

Received: January 14, 2011
Revised: March 8, 2011
Published: March 24, 2011

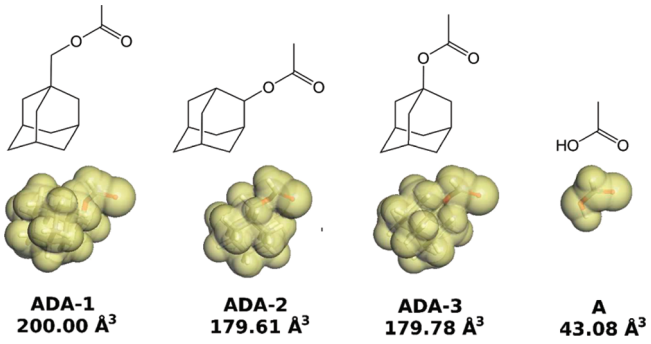

Figure 1. Structure and molecular volumes of the adamantyl ester groups used as pendant groups in this paper. Also, the molecular volume of COOH is included.

However, to our knowledge, the gas transport properties of adamantyl containing polyimides have not yet been reported. Thus, the main goal of this work has been to study the gas separation properties of novel adamantyl containing copolyimides.

Up to present, all polyimides having adamantane units have been synthesized by low-temperature solution polycondensation from a diamine or dianhydride containing the adamantyl moiety.[3−16] In this paper, the incorporation of the adamantane groups has been done by chemical modification (esterification) of a functionalized copolyimide having carboxylic acid groups which was reacted with adamantyl alcohols to yield adamantyl ester copolyimides (**PI-ADAs**). This approach is clearly more convenient to attach different pendant groups on starting from a common moiety. Particularly, we have selected three adamantane−alcohols that yielded the adamantanyl ester groups depicted in Figure 1.

The work deals with the synthesis and characterization of the novel series of copolyimides (**PI-ADAs**) and with the study of the effect of the adamantane groups in some polyimide properties such as solubility and thermal stability. In addition, the gas separation properties of these new copolyimides are studied. In order to establish the effect of the adamantane groups on these properties, the results were compared with the gas separation properties of the starting copolyimide with carboxylic acid groups. The gas transport behavior was explained by attending to some physical membrane properties and also by a computational simulation study.

EXPERIMENTAL SECTION

Materials. Carboxylic acid functionalized copolyimide (**PI-A**, Figure 3) was synthesized from 2,2-bis(3,4-dicarboxyphenyl) hexafluoropropane dianhydride, 4,4′-oxidianiline and 3,5-diaminobenzoic acid as previously described.[17]

1-Adamantane methanol (**ADA-1**), 2-adamantanol (**ADA-2**), and 1-adamantanol (**ADA-3**) were purchased from Aldrich and used as received.

Other solvents, anhydrous *N*-methylpyrrolidinone (NMP) and reagents were used without further purification.

The purity of the gases employed for permeation measurements was greater than 99.5% for oxygen and methane and greater than 99% for the others.

PI-ADA Synthesis. *General Procedure.* To a three-necked 100 mL flask fitted with a funnel drop, magnetic stirrer and nitrogen inlet were added **PI-A** with an inherent viscosity of 0.52 dL/g, (4 g, 5.2 mequiv of COOH) and 50 mL of anhydrous tetrahydrofuran. After the copolyimide was dissolved, 6.24 mequiv of the corresponding adamantanol and 7.28 mequiv of *N*,*N*′-dicyclohexylcarbodiimide (DCC) were added (a gel was formed rapidly). The gel was partially dissolved by heating at 60 °C over 30 min. Then, 6.24 mequiv of 4-(*N*,*N*-dimethylamino)pyridine (DMAP), dissolved in 15 mL of anhydrous tetrahydrofuran, was added dropwise. During the DMAP addition, the gel was dissolved completely. The mixture was stirred at room temperature until a white precipitate was formed (dicyclohexylurea, DCU). The solution was filtered and the filtrate was concentrated and poured into water. The polymer precipitate was filtered and purified by dissolving in NMP and being poured into water and subsequently into chloroform and finally poured into methanol at the end to remove any trace of reactants. The copolyimide was separated by filtration, washed with boiling ethanol for 2 h, and dried in an oven at 120 °C overnight and 30 min at 250 °C both under vacuum.

Polymer viscosity, spectroscopic data, and elemental analyses are given in the following subsections.

PI-ADA-1. η_{inh} = 0.42 dL/g. ^{1}H NMR (DMSO-d_6): δ 1.27−1.93 (m, 11.25H, H_{ADA}), 3.95 (m, 1.5H, H_f), 7.25 (d, 1H, H_h), 7.48 (d, 1H, H_g), 7,76−7.98 (m, 4.75H, H_a, H_b, H_d), 8.19 (m, 3.5H, H_c, H_e).

FT-IR (film, cm^{-1}): ν 2909 and 2850 (C−H), 1786 (C═O), 1722 (C═O), 1600 (N−C═O), 1502, (Ar C−C), 1455 (CH_2), 1348 (C−N−C), 1238 (C−O−C), 1211, 1189 (C−F), 1145, 1090 (CH), 981,960, 850, 719 (Ar−C−H).

Anal. Calcd for [$(C_{37}H_{26}N_2O_6F_6)_{0.75}(C_{31}H_{14}N_2O_5F_6)_{0.25}$, M_w = 683.15 g/mol]: C, 62.35; N, 4.09; H, 3.39. Found: C, 62.08; N, 4.21; H, 3.66.

PI-ADA-2-. η_{inh} = 0.56 dL/g. ^{1}H NMR (DMSO-d_6): δ 1.27−2.07 (m, 11.25H, H_{ADA}), 5.14 (m, 0.75H, H_f), 7.25 (d, 1H, H_h), 7.48 (d, 1H, H_g), 7,76−7.96 (m, 4.75H, H_a, H_b, H_d), 8.24 (m, 3.5H, H_c, H_e).

FT-IR (film, cm^{-1}): ν 2931 and 2861 (C−H), 1790 (C═O), 1726 (C═O), 1597 (N−C═O), 1505, (Ar C−C), 1453 (CH_2), 1357 (C−N−C), 1241 (C−O−C), 1204, 1187 (C−F), 1145, 1091 (CH), 983, 956, 843, 741, 714 (Ar−C−H).

Anal. Calcd for [$(C_{36}H_{24}N_2O_6F_6)_{0.75}(C_{31}H_{14}N_2O_5F_6)_{0.25}$, M_w = 672.64 g/mol]: C, 61.99; N, 4.16; H, 3.22. Found: C, 61.82; N, 4.28; H, 3.31.

PI-ADA-3. η_{inh} = 0.37 dL/g. ^{1}H NMR (DMSO-d_6): δ 1.10−1.81 (m, 11.25H, H_{ADA}), 7.25 (d, 1H, H_h), 7.51 (d, 1H, H_g), 7.75 (m, 2.75H, H_b, H_d), 7.97−8,35 (m, 5.5H, H_c, H_e, H_a).

FT-IR (film, cm^{-1}): ν 2936 and 2850 (C−H), 1785 (C═O), 1720 (C═O), 1591 (N−C═O), 1499, (Ar C−C), 1453 (CH_2), 1354 (C−N−C), 1241 (C−O−C), 1204, 1193 (C−F), 1145, 1091 (CH), 983, 962, 843, 746, 715 (Ar−C−H).

Anal. Calcd for [$(C_{36}H_{24}N_2O_6F_6)_{0.75}(C_{31}H_{14}N_2O_5F_6)_{0.25}$, M_w = 672.64 g/mol]: C, 61.99; N, 4.16; H, 3.22. Found: C, 60.77; N, 4.93; H, 3.51.

Membrane Preparation. Dense membranes were prepared from all **PI-ADAs** and from copolyimide precursor **PI-A** by casting 10% (w/v) filtered NMP solutions of polymers onto a glass plate and heating at 60 °C overnight. The films were stripped off from the glass plate and they were dried in an oven under vacuum following the next protocol: 120 °C/12 h, 180 °C/8 h, 250 °C/3 h, and 300 °C/30 min. The absence of residual solvent was confirmed by TGA. Film thicknesses were 55−75 μm.

Characterization. ^{1}H NMR spectra were recorded on a Varian Gemini 300 spectrometer operating at 300 MHz. Infrared attenuated total reflection (FTIR-ATR) spectra of polymer films were recorded on a Perkin-Elmer RX-1 instrument. The polymer solubility was determined by mixing 10 mg of polymer with 1 mL of solvent for 24 h at room temperature. Samples that were not soluble were heated to solvent boiling temperature. Microanalyses were made with a Carlo Erba EA1108 elemental analyzer. Inherent viscosities were measured at

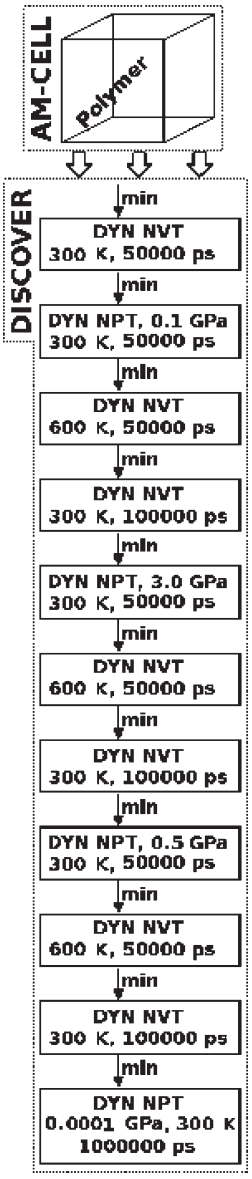

Figure 2. Molecular dynamics protocol employed in this work.

25 °C with an Ubbelohde viscosimeter using NMP as solvent at 0.5 g/dL concentration. Thermogravimetric analysis (TGA) data were recorded on TA Q-500 analyzer under nitrogen atmosphere, using around 5 mg of sample. The Hi-Res Dynamic method was used, so that the heating rate was automatically adjusted in response to changes in the rate of weight loss, which resulted in improved resolution. Differential scanning calorimetry (DSC) data were obtained on a TA DSC Q2000 from around 5 mg samples at a 20 °C/min scanning rate under a flow nitrogen atmosphere of 50 mL/min.

Densities were measured in a density balance by weighting the samples in air, w_{air}, and then in a liquid of known density (isooctane), w_{liquid}. The density of the sample was calculated from the expression $\rho_{sample} = \rho_{liquid}\,((w_{air} - w_{liquid})/w_{air})$. The density data were used to evaluate chain packing by calculating the experimental fractional free volume (FFV^{EXP}), which was estimated using the following relation: $FFV^{EXP} = (V_{sp} - 1.3V_{vdW}{}^{SU})/V_{sp}$, where V_{sp} is the polymer specific volume and $V_{vdW}{}^{SU}$ is the van der Waals volume of a structural unit, which was given by the Hyperchem computer program, version 7.0.[18]

Wide angle X-ray scattering diagrams were performed on polymer films using a Bruker D8 Advance system provided with a Vantec 1 detector. Cu Kα radiation of wavelength 1.54 Å was used, operating at 40 kV and 40 mA. The angular range was 1−50°.

Gas Transport Properties. A barometric permeation method was used to determine steady state pure gas permeability at 30 °C. The downstream pressure was kept below 10^{-2} mbar, while the upstream pressure was maintained at 3 atm. For permeation experiments, pure helium (to check the absence of pinholes), oxygen, nitrogen, methane and carbon dioxide were used. Permeability values (P) were determined from the slope of downstream pressure versus time plotted once steady state had been achieved according with the expression

$$P = K(B \times L)/P_0$$

where K is an apparatus constant that joined some parameters such as temperature, cell area permeation and volume of the system, B is the slope of downstream pressure versus time, L is the film thickness, and P_0 is the upstream pressure.

Gas diffusivities (D) were estimated from time-lag data (θ), using the relation

$$D = L^2/6\theta$$

where L is the thickness of the polymer film.

Apparent solubility coefficients, S, were estimated using the following relation:

$$S = P/D$$

For the plasticization study, the CO_2 upstream pressure was varied from 1 to 30 bar.

Computational Simulation. The study has been carried out using a single chain of the polymer model containing 24 structural units (18/6). Fifteen structures were built for each copolymide, being the results the average of these structures. The molecular dynamics method has been performed, by using the computational package Materials Studio (MS)[19] and the free volume properties of these structures has been studied using the MS package and the group contribution algorithm FVrand.[20] For the study we have used specifically two modules: Amorphous Cell, to build a polymer box at low density (0.01 g/cm^3) and Discover, to apply a collection of *NVT* and *NPT* molecular dynamics in order to obtain an optimized polymer box with the experimental density. The molecular dynamics protocol is similar to those employed by Hofmann et al. and it is detailed in Figure 2.[21] Structures have been simulated using the PCFFforce field.[22,23]

Theoretical FFV (FFV^{th}) has been calculated using the following relation: $FFV^{th} = (V_{BOX} - 1.3V_{vdW}{}^{box})/V_{BOX}$, where V_{BOX} is the volume of the optimized polymer box and $V_{vdW}{}^{box}$ is the van der Waals volume calculated by the MS package.

FFV has been also calculated using the group contribution algorithm FVrand (FFV^{FVrand}) by means of the Montecarlo method. FVrand also calculates the free volume distribution (FVD) of the polymer by the insertion of test particles. The FVD calculated by FVrand is the distribution in size of test particles whose volume is bigger than those of a sphere with a radius of 1.2 Å.

The FVD of the system can be used to estimate gas diffusion coefficients by comparison with the total volume of test particles whose volume is bigger than the "ideal kinetic volume" of each gas (IKV, volume calculated using the kinetic radius of a gas and considering this gas as an sphere: IKV(CO_2)= 17.64 Å^3, IKV(O_2)= 21.13 Å^3, IKV(N_2)= 25.25 Å^3, and IKV(CH_4)= 30.35 Å^3); this volume will be referred to as the exclusion fractional free volume (FFV^{EXC}).

RESULTS AND DISCUSSION

Synthesis and Characterization of PI-ADAs. The incorporation of the adamantane groups into the precursor copolyimide (**PI-A**) to yield **PI-ADA-1**, **PI-ADA-2**, and **PI-ADA-3** was

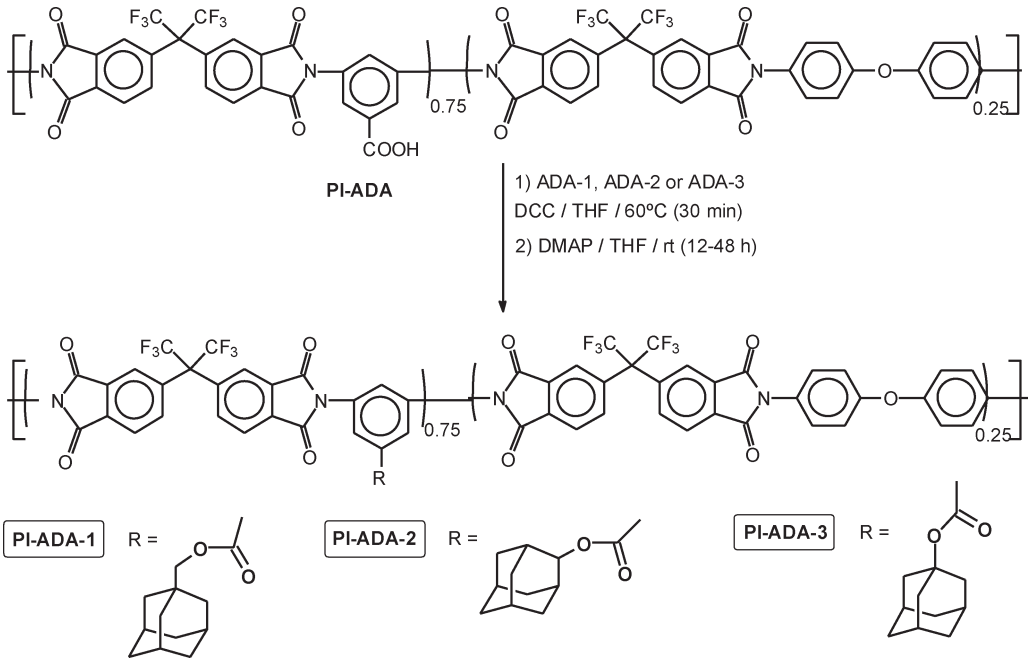

Figure 3. Synthesis and designation of **PI-ADAs** copolyimides.

carried out by esterification of **PI-A** using DCC and DMAP to activate carboxylic acids and the corresponding adamantanol in anhydrous THF (Figure 3). As it was previously reported, DCC must be first mixed with **PI-A** and the alcohol derivative until a gel is formed.[17] By this method, after adding DMAP the gel dissolves and the esterification proceeds at room temperature. Following this procedure with the current adamantanols, a gel that did not dissolve after the DMAP addition was obtained, which decreased the esterification yield. However, if the gel was first heated at 60 °C over 30 min and then DMAP was added, a clear solution was attained and reaction progressed at room temperature. Because of reactivity differences between the three alcohols, each reaction was stirred for different times. Thus, the esterification reaction of **PI-A** with **ADA-1** was stirred for 12 h while the synthesis of **PI-ADA-2** and **PI-ADA-3**, required around 24 and 48 h of reaction, respectively, to get full conversion.

The fully incorporation of the adamantane groups and the structure of the novel copolyimides were confirmed by ^{1}H NMR (Figure 4). The aromatic region of all spectra showed two signals at 7.2 and 7.4 ppm corresponding to protons *h* and *g* of the oxidianiline moiety respectively and a group of signals between 7.7 and 8.2 ppm that are due to the protons of the other phenyl moieties. However, the aliphatic regions showed remarkable differences for the three copolyimides. Thus, the protons of the $-CH_2-$ and $-CH-$ groups that linked the adamantane units to the carboxylic acid groups (protons *f*) appeared at 3.9 ppm in the **PI-ADA-1** spectrum and at 5.1 ppm in the spectrum of **PI-ADA-2**. Both spectra exhibited also a group of signals between 1.2 and 1.9 ppm, which was attributable to the protons of the adamantane moieties. **PI-ADA-3**, which has the adamantane unit directly connected from the position 1 to the carboxylic acid groups, exhibited only the group of signal between 1.10 and 1.81 ppm due to the protons of the adamantane groups.

After the modification no signal of carboxylic protons were detected in the ^{1}H NMR spectra which indicated a complete esterification of the carboxylic acid groups. The modification degrees were further confirmed by signals integration. In the case of **PI-ADA-1** and **PI-ADA-2**, estimation was done by comparing the areas between the signals of protons *h* and *f*. Thus, for **PI-ADA-1** gave a value of 1.5 and for **PI-ADA-2** the *f* /*h* ratio was 0.75, indicating a 100% of modification for both cases. For **PI-ADA-3** the area of proton *h* was compared with the area of the signal corresponding to adamantane protons. In this case the ratio was around 11 which corresponded also to a complete modification.

The FTIR spectra of all polymers were comparable. As an example, Figure 5 shows the spectrum of **PI-ADA-2**. The bands of the imide group appeared at 1785−1790 cm^{-1} (asymmetric stretching vibration of C═O), 1720 cm^{-1} (symmetric stretching vibration of C═O), 1350 (asymmetric stretching vibration of C−N), and 715 cm^{-1} (deformation of the imide ring). The carbonyl stretching of the pendant groups was partially overlapped by the absorption of the imide rings.

As has been reported by several researchers, the characteristic vibrational bands of adamantane moieties are the CH stretching band at 2900 cm^{-1}, CH_2 scissoring around 1450 cm^{-1}, and CH_2 rocks, wags and twists in the range of 1400−1000 cm^{-1}.[24,25] Excepting the CH stretching band at 2900 cm^{-1}, and two bands of low intensity at 1041 and 1283 cm^{-1}, most of the bands attributed to adamantane groups appear also in the IR spectrum of the starting polyimide, **PI-A**, which is depicted also in Figure 5. This indicated that most of the adamantane vibrational bands were overlapped by the characteristic bands of polyimides.

The elemental analyses of all polymers were also in good agreement with the calculated values for the proposed structures indicating enough purity for the synthesized copolyimides (see Experimental Section).

Inherent viscosities were moderate, between 0.37 and 0.56 dL/g. However, all copolyimides showed good film-forming ability, which made them suitable to be tested as gas separation membranes.

Polymer Properties. *Solubility and Crystallinity.* The solubility of the adamantyl ester-containing copolyimides was evaluate

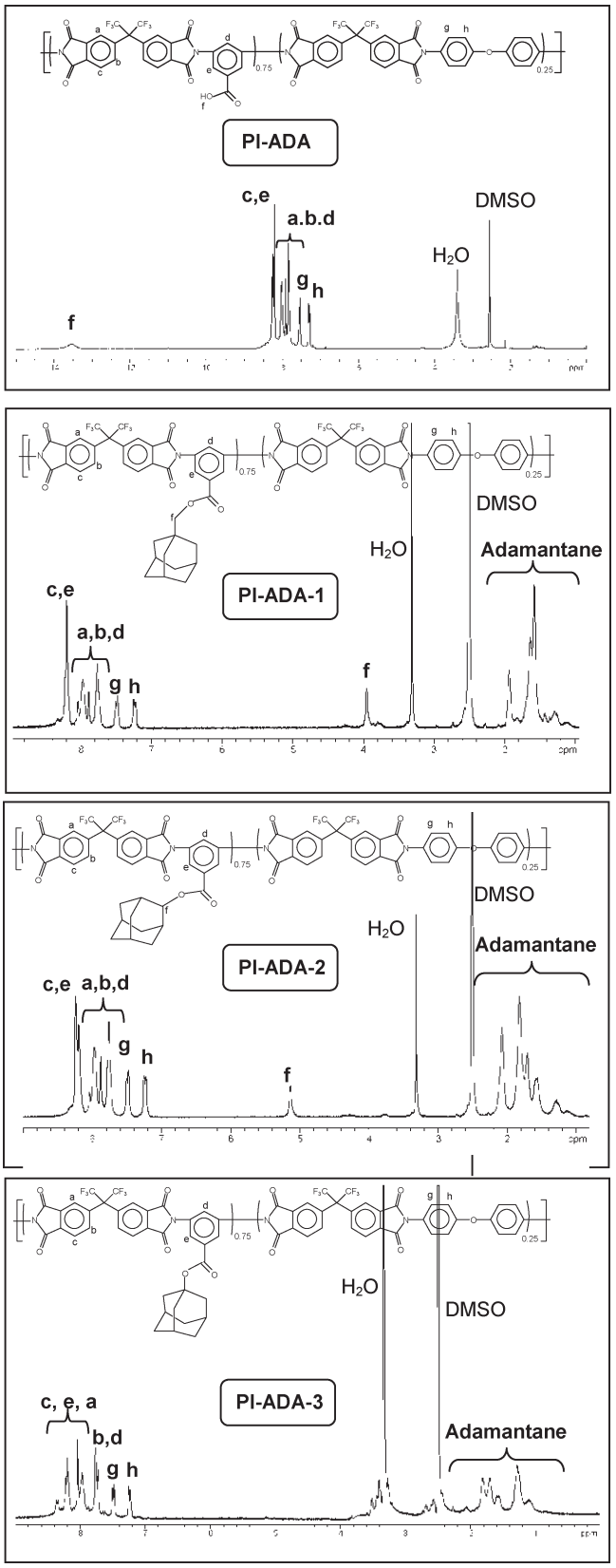

Figure 4. ^{1}H NMR spectra of **PI-A** and **PI-ADAs** copolyimides.

and compared with **PI-A**. The four copolyimides readily dissolved in polar aprotic solvents such as NMP, *N*,*N*-dimethylacetamide,

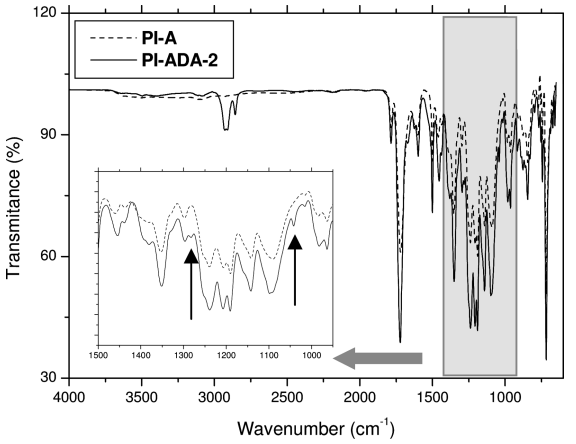

Figure 5. IR-ATR spectra of **PI-A** and **PI-ADA-2** films.

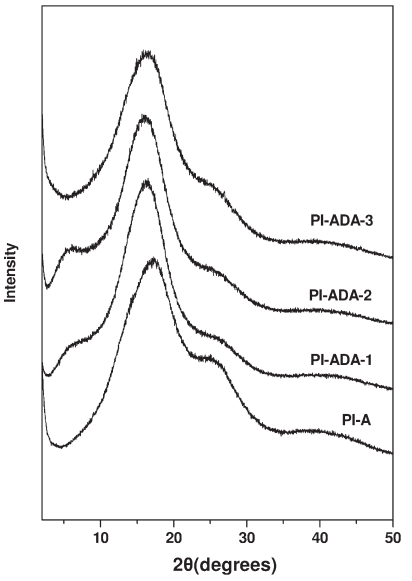

Figure 6. X-ray diffractograms (vertically shifted) of **P-ADAs** and **PI-A** films.

dimethyl sulfoxide, *N*,*N*-dimethylformamide, protic solvents such as *m*-cresol, cyclic ethers such as tetrahydrofuran and 1,4-dioxane or even in more common organic solvents such as acetone at room temperature. **PI-ADAs** were dissolved even in chlorinated solvents such as dichloromethane and chloroform. The better solubility of modified copolyimides can be attributed to the replacement of OH groups by the adamantane units, which disrupts the intermolecular attraction forces in the polymer. The solubility in aqueous alkali solution (0.1 M NaOH) was also investigated. Thus, **PI-A** was easily soluble in the NaOH solution whereas **PI-ADAs** were completely insoluble which seems to confirm that −COOH group of **PI-A** were successfully converted into ester groups by the modification reaction.

X-ray diffractograms of the **PI-ADA** films and the starting polyimide (Figure 6) showed typical halos of amorphous polymers. The starting polyimide **PI-A** presented a broad peak centered at $2\theta = 17.16°$ and a shoulder centered at $2\theta = 26°$ which corresponds to intermolecular distances of 5.13 and 3.54 Å respectively. This shoulder, that could be assigned to $\pi-\pi$ stacking of imide and phenyl rings in ordered domains,[26] decreases with the presence of

Table 1. Thermal Properties of of PI-ADA and PI-A Films

copolyimide	T_g (°C)	$T_{d_{onset}}$ (°C) (1st step)	$T_{d_{onset}}$ (°C) (2nd step)	$T_{d_{onset}}$ (°C) (3rd step)	char yield (%) at 800 °C
PI-A	335	440	520		40
PI-ADA-1	268	420	525		46
PI-ADA-2	294	410	480	530	46
PI-ADA-3	278	390	475	530	46

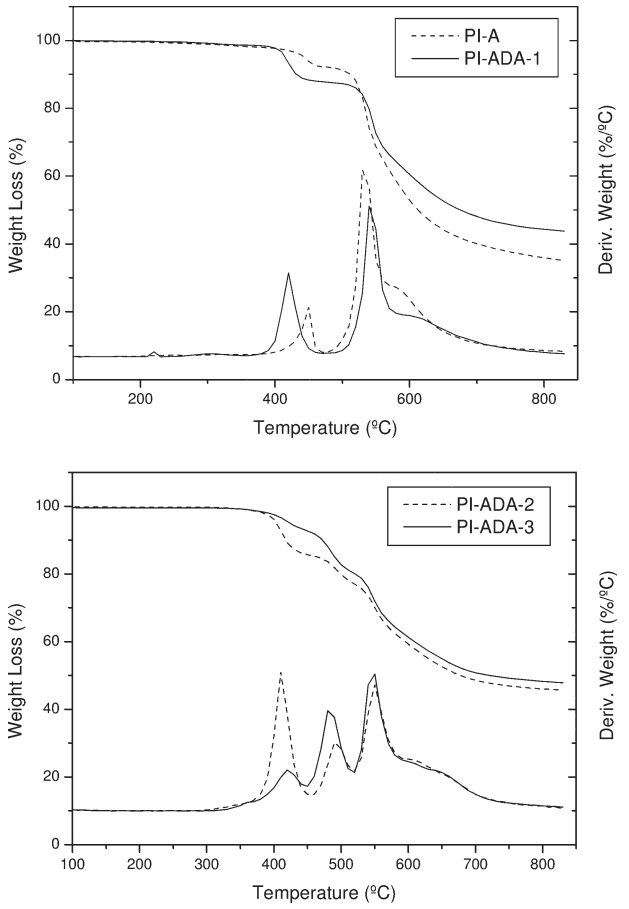

Figure 7. (Up) TGA of **PI-A** and **PI-ADA-1**. (Down) TGA of **PI-ADA-2** and **PI-ADA-3**.

the adamantane side groups. The position of the maximum at 17.16° for **PI-A** shifted to a lower position, $2\theta = 16.15°$ (d-space =5.44 Å) in the **PI-ADA** films. Besides, the amorphous halo of the **PI-ADA** films exhibited also some asymmetry on the low-angle side, which may be interpreted as a contribution of larger intersegmental distances to the global scattering pattern. All these results confirm that incorporation of adamantane groups into the polyimide brings about an increase of the intermolecular distances which is going to influence the properties in the solid state, such as T_g or FFV.

Thermal Properties. The thermal behavior of these polymers was evaluated by DSC and TGA. All modified copolyimides showed glass transition temperatures between 268 and 295 °C (Table 1), which are lower than that of **PI-A** (330 °C),.[17] The depression of the T_g can be attributed to the nonpolar character and bulkiness of the pendant groups, that reduce the intermolecular attraction forces in the polymer and produces a chain separation effect. In this regard, it has been reported that the transition from polar to nonpolar groups results in a decrease in T_g due to the reduction of the intermolecular attraction forces in the polymer.[27] On the other hand, it is well established that the bulkiness of the pendant substituents plays an important role in the T_g reduction by a chain separation effect.[28]

As to the thermal stability, **PI-ADA-1** showed two degradation steps, as the starting copolyimide **PI-A** did (Figure 7 up), while **PI-ADA-2** and **PI-ADA-3** showed three decomposition steps (Figure 7 down). The first degradation step of **PI-ADA-1**, occurred at around 420 °C and the experimental weight loss fitted well with the theoretical content of 0.75 repeat units modified with the adamantyl methylene ester pendant groups. The degradation temperature of this pendant group was lower than that of the carboxylic acid groups of **PI-A**. The second degradation step of **PI-ADA-1** took place at 525 °C and it can be ascribed to the generalized polymer decomposition. From these results, the conclusion can be drawn that when adamantane is linked to the polyimide through a methylene ester moiety, the thermal stability slightly decreases when compared with the starting copolyimide. This result was in agreement with other copolyimides wearing ester pendant groups.[28]

The adamantanyl ester groups of **PI-ADA-2** and **PI-ADA-3**, seemed to degrade in two stages: at 410 and 480 °C in **PI-ADA-2** and, at slightly lower temperatures in **PI-ADA-3** (390 and 475 °C). In the case of **PI-ADA-2** the experimental weight loss of the first step (14.25%) fitted well with the theoretical weight of the adamantane unit (14.81%). The experimental weight loss of second step was around 6% and could be attributed to the loss of the carboxylate groups. So, it can be presumed that the degradation of **PI-ADA-2** started with the decomposition of the whole adamantane group followed by a decarboxylation process. However, in the case of **PI-ADA-3** the experimental weight loss of the first step was around 7%, lower than the theoretical weight loss corresponding to the whole adamantane unit (14.81%). It suggested that degradation of the pendant group of **PI-ADA-3** was a more complicate process, that started with a partial degradation of the adamantane group. Both copolymers showed also a large third decomposition step at 530 °C associated with the generalized polymer degradation.

Thus, it can be stated that, depending on the adamantanol used in the esterification reaction, different degradation patterns were obtained. Disappointingly, at this moment, a plausible degradation mechanism cannot be advanced.

Also, char yield at 800 °C of these copolymers were very similar, which means that no matter the degradation pattern is, the current modified polyimides completely lose the adamantyl ester group leading to the same material at very high temperature.

Gas Separation Properties. *Pure-Gas Permeation.* Permeability coefficients (P) to O_2, N_2, CH_4 and CO_2 were measured on polymer films and data are listed in Table 2. To establish the effect of the adamantane groups, the results were compared with the gas separation properties of the precursor copolyimide (**PI-A**). Gas transport properties of **PI-A** has been previously reported by us;[17] nevertheless, to compare the results properly, we have measured the gas separation properties from a new membrane of this copolymer

Table 2. Permeability (*P*, Barrers[a]), Diffusion Coefficient ($D \times 10^8$ cm^2/s), Solubility Coefficient ($S \times 10^3$ cm^3/STP/cm^3 cmHg), and Selectivity Coefficients of PI-ADA and PI-A films

membrane	parameter	O_2	N_2	CH_4	CO_2	O_2/N_2	CO_2/N_2	CO_2/CH_4
PI-A	*P*	1.52	0.26	0.13	5.41	5.84	20.80	41.6
	D	1.19	0.34	0.11	0.32	3.50	0.94	2.90
	S	12.7	7.64	11.8	169	1.66	22.12	14.32
	P	3.79	0.72	0.39	14.39	5.26	19.98	36.8
PI-ADA-1	*D*	4.89	1.50	0.20	1.51	3.26	1	7.55
	S	7.7	4.8	19.5	95	1.6	19.79	4.8
	P	4.79	0.83	0.45	16.06	5.77	19.34	35.7
PI-ADA-2	*D*	4.51	1.33	0.17	1.42	3.39	1.06	8.35
	S	10	6.2	26.4	113	1.6	18.2	4.2
	P	3.23	0.67	0.37	12.93	4.82	19.29	34.9
PI-ADA-3	*D*	2.50	0.82	0.15	1.14	3.04	1.39	7.6
	S	12.9	8.17	24.6	113	1.5	13.8	4.6

[a] 1 barrer $=10^{-10}$ cm^3 (STP) cm/cm^3 s cmHg.

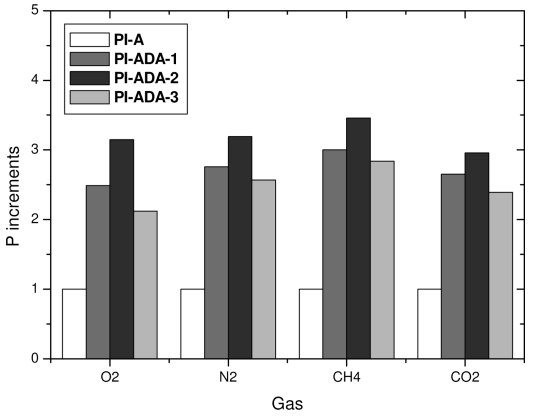

Figure 8. Permeability coefficient increments of **PI-ADAs** compared with **PI-A**.

that was thermally treated under identical conditions that **PI-ADAs** copolyimides.

All **PI-ADA** copolyimides showed higher permeability coefficients (2 or 3 times higher) than the copolyimide precursor, depending on the gas tested, as it is depicted in Figure 8. This result confirmed that pendant adamantane groups were adequate to increase the permeability coefficients of polyimides. **PI-ADA-2** was slightly more permeable than **PI-ADA-1** and **PI-ADA-3**, which showed similar gas transport properties.

As *P* can be split into a kinetic parameter, *D* (diffusion coefficient), which can be associated with the structure of the polymer, and a thermodynamic parameter, *S* (solubility coefficient), that can be associated with the gas-polymer interactions, but parameters have been evaluated to explore their contribution to the increases of permeability (Table 2). The diffusion coefficients of all **PI-ADA** membranes were higher than that of the corresponding **PI-A** while solubility coefficients were similar (Figure 9).

The increments of *D* were probably due to the gain of fractional free volume (FFV) brought about by the bulkiness of the adamantane groups that in the **PI-ADA** membranes. The presence of adamantyl groups, and their effect on the FFV, can be

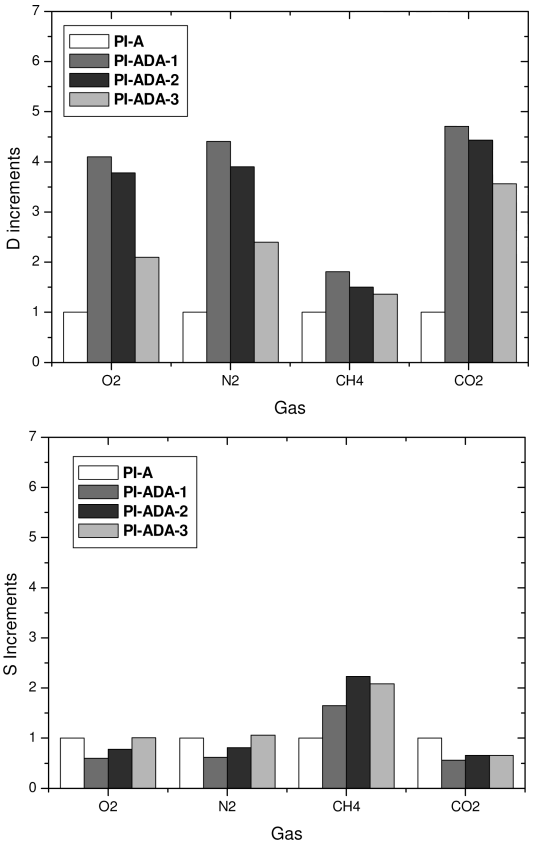

Figure 9. (Up) Diffusivity coefficients increments of **PI-ADAs** compared with **PI-A**. (Down) Solubility coefficients increments of **PI-ADAs** compared with **PI-A**.

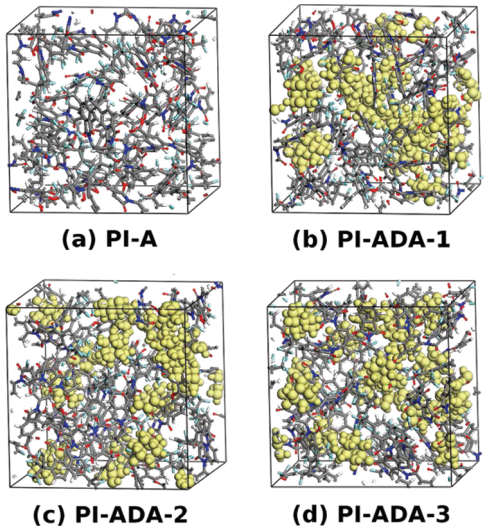

Figure 10. Optimized polymer boxes after the molecular dynamics simulation. The adamantyl pendant groups are marked in yellow.

visually appreciated in Figure 10, where the theoretically simulated polymer boxes are represented with the adamantyl pendant groups marked in yellow.

The theoretical calculations allowed to determine the theoretical FFVth, the theoretical density ρ^{th}, and FV^{rand}, which is the theoretical FFV calculated by using a novel algorithm recently

Table 3. Physical and Theoretical Properties of PI-ADA and PI-A films

membrane	ρ^{EXP} (g/cm^3)	ρ^{th} (g/cm^3)	V_{sp}(cm^3/g)	FFV^{EXP} [a]	FFV^{th} [a]	FFV^{FVrand} [a]
PI-A	1.4939	1.540	0.669	0.163	0.183	0.232
PI-ADA-1	1.3844	1.343	0.722	0.170	0.223	0.276
PI-ADA-2	1.3830	1.358	0.723	0.177	0.217	0.269
PI-ADA-3	1.3974	1.454	0.715	0.166	0.209	0.266

[a] Experimental FFV(FFV^{EXP}) and theoretical FFVs(FFV^{th} and FFV^{rand}).

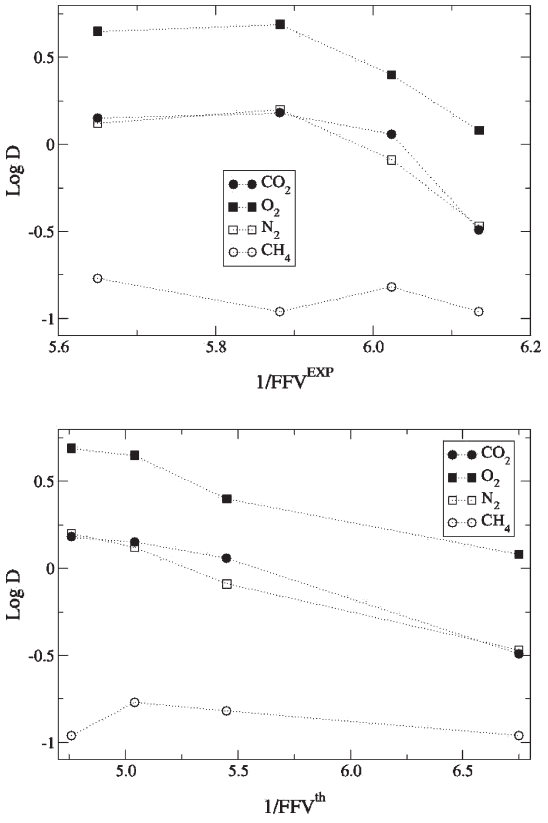

Figure 11. Relationship between log D and $1/FFV^{EXP}$ (up) and log D and $1/FFV^{th}$ (down).

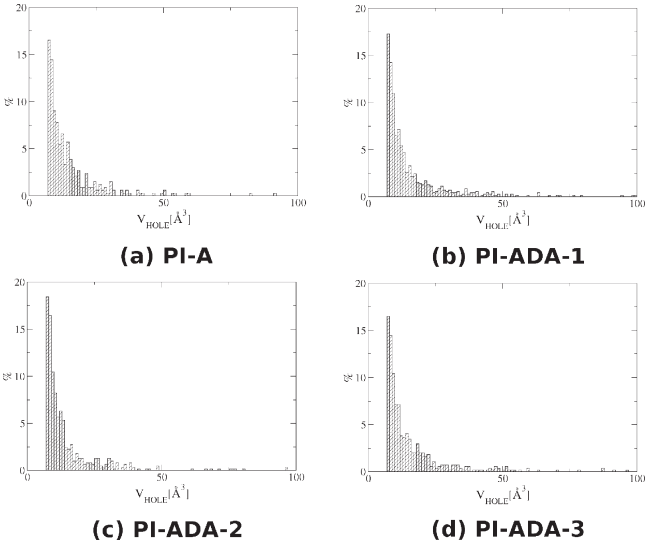

Figure 12. FVD of the four polymers calculated using FVrand. The y-axis represents the percentage of total free volume for each range of hole volumes (V_{HOLE}).

developed in our group.[20] This permit to make a comparative study of the molecular simulation tools as the experimental FFV (FFV^{EXP}) could be evaluated from the experimental density ρ^{exp} (Table 3). The theoretical densities present a qualitative correspondence with the experimental ones, observing the same tendency except for the case of **PI-ADA-1** and **PI-ADA-2**, where the values are inverted. However, the densities of these two copolyimides are so alike that the simulated structures should still correspond to the experimental ones within the error range.

Both FFV^{EXP} and FFV^{th} of all **PI-ADAs** membranes were higher than those of **PI-A** which confirmed the positive effect of adamantane groups on reducing the molecular packing and therefore increasing the permeability and diffusion coefficients. Attending to the theoretical FFV, it can be seen that the FVrand algorithm overestimates the FFV in approximately a 25% of FFV^{th} but it follows the same trend. FFV^{EXP} followed also the same trend as permeability, that is: FFV^{EXP} (**PI-ADA-2**) > FFV^{EXP} (**PI-ADA-1**) > FFV^{EXP} (**PI-ADA-3**) > FFV^{EXP} (**PI-A**). On the other hand, FFV^{th} followed the same trend as diffusivity: FFV^{th} (**PI-ADA-1**) > FFV^{th} (**PI-ADA-2**) > FFV^{th} (**PI-ADA-3**) > FFV^{th} (**PI-A**). If gas permeation was governed by FFV, a linear relationship between log D and 1/FFV should be found.[29] In the case of FFV^{EXP} (Figure 11 up) the relationship was not totally linear, but with FFV^{th} an almost linear relationship could be found for all the gases except CH_4 (Figure 11 down). This indicated that gas permeation should be mainly governed by FFV in this series of copolyimides.

In order to estimate the diffusion coefficients for the four copolyimides, the FVDs were calculated and the results are shown in Figure 12. Although the shape of the distribution is similar for the four cases, it can be observed that **PI-ADAs** polymers present more free volume elements of volume bigger than 50 Å^3: a total of 10 free volume elements for the 15 **PI-A** simulated structures, 20 elements for the **PI-ADA-1** structures, 22 for the **PI-ADA-2** structures and 25 for the **PI-ADA-3** structures. This fact could be responsible of the observed FFV differences.

Once the FVDs were built, the experimental D of the four gases studied can be compared with the exclusion fractional free volumes (FFV^{EXC} or total volume of holes that are bigger than the ideal kinetic volume of each gas) as shown in Figure 13, where the FFV^{EXC} values have been normalized for a better comparison with D.

Comparing the values of FFV^{EXC} and experimental D for each gas and each polymer (Figure 13, left), a qualitative correlation can be seen for all the gases except CH_4. This lack of correlation for this condensable gas suggested that better results could be

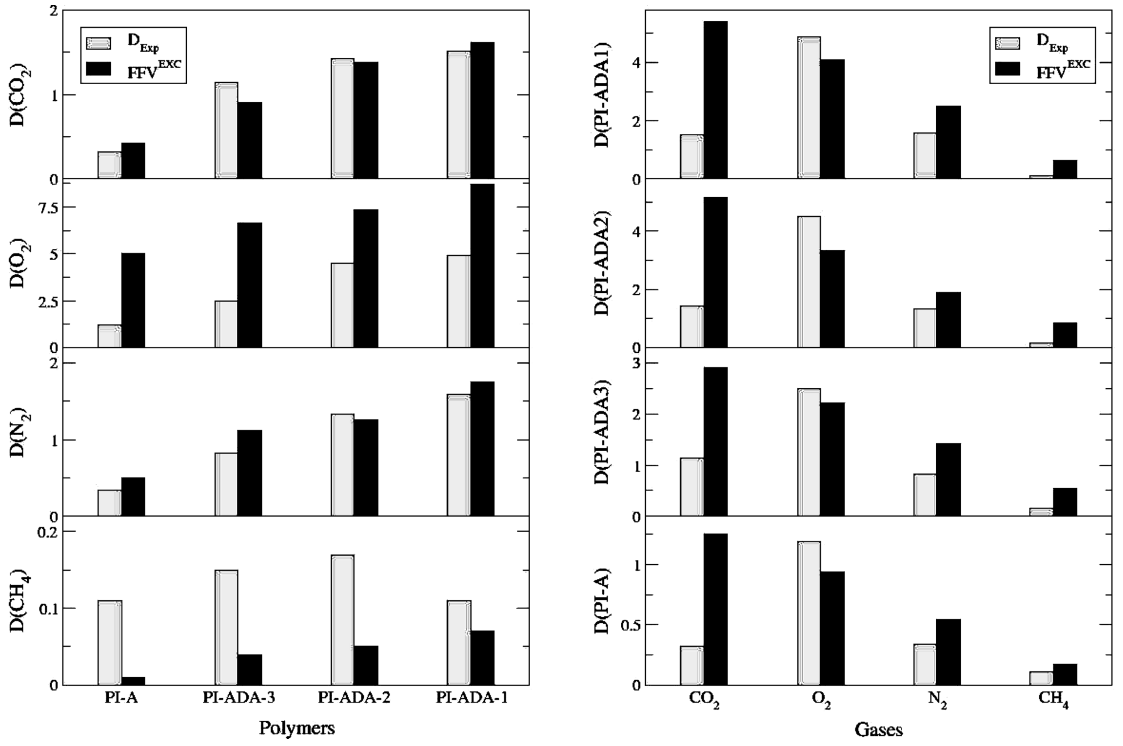

Figure 13. Representation of the experimental D (D_{EXP}, gray bars, $D \times 10^8$ cm^2/s) and the normalized FFV^{EXC} (black bars, [FFV^{EXC} − min (FFV^{EXC}) + min(D_{EXP})][max(D_{EXP}) − min(D_{EXP})]/[max(FFV^{EXC})) − min(FFV^{EXC})]) for the four polymers and four gases. D_{EXP} and FFV^{EXC} are represented as a function of the polymers (left) and as a function of the gases (right).

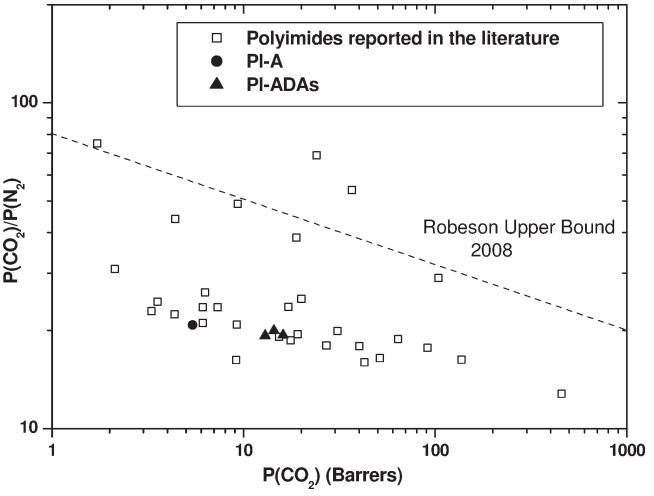

Figure 14. Performance of **PI-ADAs** for CO_2/N_2 separations compared with **PI-A** and with other polyimides reported in the literature.

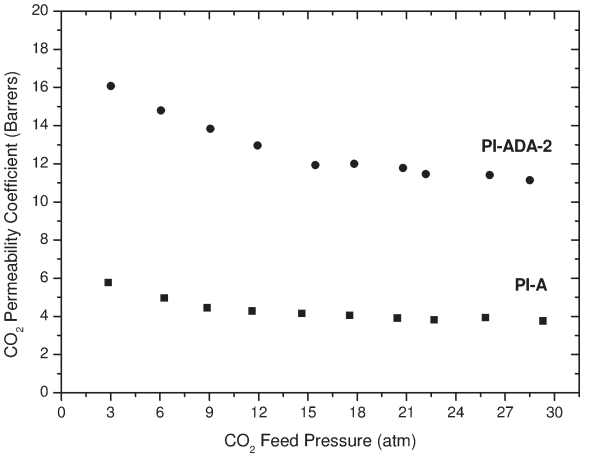

Figure 15. CO_2 permeability-feed pressure curves of **PI-ADA-2** and **PI-A** films.

achieved by using bigger polymer models. The correlation of FFV^{EXC} and D for the same polymer as a function of the gas (Figure 13, right) is nonexistent for the case of CO_2, which gives similar results than those of N_2 in terms of free volume; this is due because CO_2 is also a condensable gas with a low ideal behavior. However, that relationship is still qualitative for the other three gases. The differences in gas permeation between polymers can be justified in terms of free volume but this is not enough to estimate the capability of a polymer to discriminate between gases. This will be commented more in depth in the next section.

As to the solubility coefficients, it is to remark that, as a rule, they were lower for the modified polymers than those of the original **PI-A**. An exception of this rule was CH_4, which showed significant increments of solubility on passing from **PI-A** to adamantyl-containing polyimides (see Table 2 and Figure 9). This effect should be considered as consistent because of the aliphatic nature of both CH_4 and adamantane. One can presume also that the particular affinity of CH_4 for the **PI-ADAs** is the responsible of the selectivity loss observed for CO_2/CH_4, which was more pronounced than for O_2/N_2 and CO_2/N_2, respect to the starting **PI-A**.

dx.doi.org/10.1021/ma200093j |*Macromolecules* 2011, 44, 2780–2790

Selectivity. Ideal selectivities of O_2/N_2, CO_2/N_2, and CO_2/CH_4 pairs are listed in Table 2.

O_2/N_2 selectivities of **PI-ADA** films were acceptable, but not especially high, ranging from 4.82 to 5.77. The O_2/N_2 selectivity of **PI-ADA-2** was not seriously affected since it decreased 1.2% respect to **PI-A** but, selectivities of **PI-ADA-1** and **PI-ADA-3** were 10 and 17% respectively, lower than that of **PI-A.**

CO_2/CH_4 selectivities of **PI-ADAs** films were lower than that of **PI-A**, between 11 and 16% lower, but they were still near 40, which is the upper limit of most of the reported 6FDA-copolyimides.[30] This result suggested that **PI-ADAs** films could be efficiently employed to perform this separation.

CO_2/N_2 selectivities of **PI-ADA** films were close to 20 and only diminished 4−7% respect to the starting polyimide, so that the use of **PI-ADA** membranes seems to be more convenient than using **PI-A** to carry out CO_2/N_2 separations because CO_2 permeability increases between 2.3 and 3 times, while selectivity remains almost constant. As an example, performance of **PI-ADAs** films to carry out this gas separation is compared with the starting polyimide and with other polyimides reported in the literature (Figure 14).

Plasticization. A disadvantage of polyimides to be applied in technical high-pressure separations, such as natural gas upgrading or enhanced oil recovery, is their great tendency to plasticize at high CO_2 pressures.[31−33]

A typical effect of plasticization is that at low upstream pressures, the gas permeability decreases with increasing pressure going through a minimum, which is taken as the plasticization pressure. Then, when the pressure is further raised, the high CO_2 concentration in the polymer film disrupts the polymeric chain packing and enhances the segmental mobility and, as a consequence permeability raises and the polymer membrane loses its selectivity. Thus, the permeability of CO_2 as a function of CO_2 feed pressure was evaluated for the more permeable copolyimide that is **PI-ADA-2**, and for the starting polyimide **PI-A.** The results are depicted in Figure 15.

Interestingly, both copolyimides exhibited a suppression of the plasticization effect.

Plasticization of polyimides containing −COOH pendant groups, has been less studied than other materials.[34,35] Staudt-Bickel et al. attributed the absence of plasticization of these membranes to a cross-linking effect caused by hydrogen bonding between free carboxylic acid groups.[34] However, Kratochvil et al., who treated the films at high temperature (350 °C), attributed the absence of platicization to a decarboxylation process. Annealing at high temperatures can bring about the release of the pendant acid groups, which creates phenyl radicals, that on turn can attack other positions of the polyimide producing a cross-linking.[35] However, in our case the temperature and time of heat treatment, for **PI-A** film, was not enough to induce decarboxylation because this copolyimide needs thermal treatments above to 425 °C to efficiently remove the −COOH groups.[17] Moreover, it has been demonstrated that suppression of plasticization can be achieved by heat treatments at 350 °C that causes a densification of polymer matrix resulting in a reduction of chain mobility.[32] Therefore, the absence of plasticization of a **PI-A** treated at 300 °C for 30 min could be attributed to both phenomena: 1) a physical cross-linking effect caused by hydrogen bonding between free carboxylic acid groups and 2) a macromolecular matrix densification caused by thermal annealing. The absence of plasticization of the **PI-ADA-2** film was an interesting and unexpected result taking into account that after the esterification reaction no free carboxylic acid groups are present in the polymer. The absence of plasticization in this case could be attributed to the densification of the polymer matrix caused by temperature.

To confirm these assumptions **PI-A** and **PI-ADA-2** films were dipped in NMP. After 1 h **PI-ADA-2** was completely dissolved, what indicated the absence of cross-linking, whereas **PI-A** was not dissolved after 1 week in NMP. From this study, we can establish that the incorporation of adamantane groups into aromatic polyimides yielded a noncross-linked copolyimide with plasticization resistance.

CONCLUSIONS

Primary, secondary, and tertiary adamantane alcohols can be introduced in quantitative yield into copolyimides that wear free carboxylic acid pendant groups, through an esterification reaction using DCC and DMAP to activate the −COOH groups. The fully incorporation of these alcohols was confirmed by ^1H NMR, IR and elemental analysis.

The adamantyl ester pendant groups endowed **PI-ADAs** copolyimides with excellent solubility in common organic solvents and high glass transition temperatures, between 268 and 295 °C. Thermal decomposition of these copolyimides started with the loosening of the adamantyl ester group which releases at different temperatures (between 390 and 420 °C) and followed a different decomposition pattern depending on the attached adamantane group. Char yields were similar for the three **PI-ADAs** making evident that the removal of the pendant groups leads to a similar structure.

All **PI-ADA** copolyimides showed higher permeability and diffusion coefficients than the starting **PI-A**. Experimental and theoretical fractional free volume (FFV^{EXP} and FFV^{th}) data of all **PI-ADAs** membranes were higher than those of the starting copolyimide, which confirmed the positive effect of adamantane groups on reducing the molecular packing and increasing the permeability and diffusion coefficients. Thus, it was established that gas permeation was mainly governed by the FFV.

CO_2/N_2 and CO_2/CH_4 selectivity values (close to 20 and 40, respectively) suggested that **PI-ADA** membranes are materials with promising performances to carry out these separations. However, no good correlation was observed between the theoretical and experimental selectivity, which indicated that besides the free volume, other factors should be considered to explain this parameter.

In addition to the fact that the adamantane pendant group yielded copolyimides more permeable than the starting copolyimide and with reasonable selectivity, the copolyimides obtained showed an apparent absence of plasticization, as also happened with the starting copolyimide.

AUTHOR INFORMATION

Corresponding Author

*Telephone (Lab): (34) 91 562 29 00 (Ext 350). Telephone (Office): (34) 91 562 29 00 (Ext 457). Fax: (34) 91 564 48 53. E-mail: evamaya@ictp.csic.es.

ACKNOWLEDGMENT

The financial support provided by Spanish Ministerio de Ciencia e Innovación (MICINN) (MAT2010-20668) and by

MULTICAT project is gratefully acknowledged. Thanks are expressed to CTI, CSIC, for generous allocation of CPU time.

REFERENCES

(1) Ghosh, M. K.; Mittal, K. L. *Polyimides: fundamentals and applications*. New York: Marcel Dekker: 1996.
(2) Liaw, D. J.; Liaw, B. Y. *Polym. J.* **1999**, *31*, 1270–1273.
(3) Fort, R. C.; Schleyer, P. V. R. *Chem. Rev.* **1964**, *64*, 227–300.
(4) Espeso, J. F.; Lozano, A. E.; de la Campa, J. G.; García-Yoldi, I.; de Abajo, J. *J. Polym. Sci., Part A: Polym. Chem.* **2010**, *48*, 1743–1751.
(5) Chern, Y. T.; Shiue, H. C. *Macromolecules* **1997**, *30*, 4646–4651.
(6) Chern, Y. T.; Lin, K. S.; Kao, S. C. *J. Appl. Polym. Sci.* **1998**, *8*, 315–321.
(7) Chern, Y. T.; Shiue, H. C. *Macromol. Chem. Phys.* **1998**, *199*, 963–969.
(8) Chern, Y. T.; Shiue, H. C.; Kao, S. C. *J. Polym. Sci., Part A:, Polym. Chem.* **1998**, *36*, 785–792.
(9) Mathews, A. S.; Kim, I.; Ha, C.-S. *J. Polym. Sci., Part A: Polym. Chem.* **2006**, *44*, 5254–5270.
(10) Mathews, A. S.; Kim, I.; Ha, C.-S. *J. Appl. Polym. Sci.* **2006**, *102*, 3316–3326.
(11) Mathews, A. S.; Kim, I.; Ha, C.-S. *Macromol. Symp.* **2007**, *249−250*, 344–349.
(12) Hsiao, S. H.; Li, C. T. *Macromolecules* **1998**, *31*, 7213–7217.
(13) Yi, M. H.; Huang, W.; Lee, B. J.; Choi, K. Y. *J. Polym. Sci., Part A: Polym. Chem.* **1999**, *37*, 3449–3454.
(14) Liaw, D. J.; Liaw, B. Y. *Macromol. Chem. Phys.* **1999**, *200*, 1326–1332.
(15) Kwak, S. M.; Yeon, J. H.; Yoon, T. H. *Polym. Sci., Part A: Polym. Chem.* **2006**, *44*, 2567–2578.
(16) Kung, Y. C.; Liou, G. S.; Hsiao, S. H. *Polym. Sci., Part A: Polym. Chem.* **2009**, *47*, 1740–1755.
(17) Maya, E. M.; Tena, A.; Lozano, A. E.; de Abajo, J.; de la Campa, J. G. *J. Membr. Sci.* **2010**, *349*, 385–392.
(18) Hyperchem, Computational Chemistry, Version 7.0 Hypercube Inc.: Gainesville, FL, 2002.
(19) Materials Studio v4.4.0.0. © 2001−2009 Accelrys Software Inc.: San Diego, CA.
(20) García-Yoldi, I.; Lozano, A. E.; de la Campa, J. G. *Macromol. Theory Simul.* **2011**submitted for publication.
(21) Hoffmann, D.; Fritz, L.; Ulbrich, J.; Paul, D. *Comput. Theor. Polym. Sci.* **2000**, *10*, 419–436.
(22) Maple, J. R.; Dinur, U.; Hagler, A. T. *Proc. Natl. Acad. Sci. U.S.A.* **1988**, *85*, 5350–5354.
(23) Maple, J. R.; Hwang, M. J.; Stockfisch, T. P.; Dinur, U.; Waldman, M.; Ewig, C. S.; Hagler, A. T. *J. Comput. Chem.* **1994**, *15*, 162–182.
(24) Broxton, T. J.; Teady, L. W.; Kendall, M.; Topsom, R. D. *Appl. Spectrosc.* **1971**, *25*, 600–604.
(25) Jensen, J. M. *Spectrochim. Acta, Part A* **2004**, *60*, 1895–1905.
(26) Calle, M.; Lozano, A. E.; de Abajo, J.; de la Campa, J.; Alvarez, C. *J. Membr. Sci.* **2010**, *365*, 145–153.
(27) Schmaljohann, D.; Häussler, L.; Pötschke, P.; Voit, B. I.; Loontjens, T. J. *Macromol. Chem. Phys.* **2000**, *201*, 49–57.
(28) Maya, E. M.; Lozano, A. E.; de Abajo, J.; de la Campa, J. G. *Polym. Degrad. Stab.* **2007**, *92*, 2294–2299.
(29) Lee, V. M. *Polym. Eng. Sci.* **1980**, *20*, 65–69.
(30) Wind, J. D.; Koros, W. J. *J. Membr. Sci.* **2004**, *228*, 227–236.
(31) Bos, A.; Pünt, I. G. M.; Wessling, M.; Strathmann, H. *J. Membr. Sci.* **1999**, *155*, 67–78.
(32) Ismail, A. F.; Lorna, W. *Sep. Purif. Tech.* **2002**, *27*, 173–194.
(33) Lee, S. J.; Madden, W.; Koros, W. J. *J. Membr. Sci.* **2010**, *350*, 242–251.
(34) Staudt-Bickel, C.; Koros, W. J. *J. Membr. Sci.* **1999**, *135*, 145–154.
(35) Kratochvil, A. M.; Koros, W. J. *Macromolecules* **2008**, *41*, 7920–7927.